Mod Pathol 38 (2025) 100881

MODERN PATHOLOGY

USCAP UNITED STATES AND CANADIAN ACADEMY OF PATHOLOGY
Advancing Pathology Together

Journal homepage: https://modernpathology.org/

Research Article

Epstein-Barr Virus–Associated Gastric Cancer: A Histopathologic Study With Comprehensive Molecular Profiling

Valentina Angerilli[a], Jessica Gasparello[b], Antonio Collesei[c], Carlotta Ceccon[a,b], Francesca Bergamo[c], Marianna Sabbadin[a,b], Paola Parente[d], Alessandro Vanoli[e,f], Monia Niero[a], Claudio Luchini[g], Roberta Gafà[h], Angelo Paolo Dei Tos[b], Federica Grillo[i,j], Luca Mastracci[i,j], Sara Lonardi[c], Matteo Fassan[b,c,*]

[a] *ULSS2 Marca Trevigiana, Surgical Pathology Unit, Treviso, Italy;* [b] *Department of Medicine, University of Padua, Italy;* [c] *Veneto Institute of Oncology, IOV-IRCCS, Padua, Italy;* [d] *Pathology Unit, Fondazione IRCCS Ospedale Casa Sollievo della Sofferenza, Rotondo, Italy;* [e] *Department of Molecular Medicine, University of Pavia, Pavia, Italy;* [f] *Anatomic Pathology Unit, IRCCS San Matteo Hospital Foundation, Pavia, Italy;* [g] *Department of Pathology and Diagnostics, University and Hospital Trust of Verona, Verona, Italy;* [h] *Department of Translational Medicine, University of Ferrara and Anatomic Pathology Unit, Azienda Ospedaliero-Universitaria S. Anna, Ferrara, Italy;* [i] *Anatomic Pathology Unit, Department of Surgical Sciences and Integrated Diagnostics (DICS), University of Genova, Genova, Italy;* [j] *Ospedale Policlinico San Martino, IRCCS for Oncology and Neuroscience, Genova, Italy*

ARTICLE INFO

Article history:
Received 21 May 2025
Revised 25 July 2025
Accepted 7 August 2025
Available online 4 September 2025

Keywords:
biomarkers
Epstein-Barr virus
gastric cancer
molecular profiling

ABSTRACT

A subset of gastric cancers (GCs) is linked to Epstein-Barr virus (EBV) infection. This study aims to characterize the histopathological and molecular features of EBV-associated GCs (EBVaGCs), focusing on predictive biomarkers and genomic and transcriptomic analysis. A total of 35 primary EBVaGCs were considered. The presence of EBV was confirmed with in situ hybridization. Immunohistochemical analyses for HER2, PD-L1, claudin 18.2, and mismatch repair proteins were performed. Genomic and transcriptomic profiles were assessed using AmoyDx Master Panel, which can identify single-nucleotide variants, InDels, and copy number variations on 571 hot genes, as well as microsatellite status, tumor molecular burden, and homologous recombination deficiency at the DNA level; however, at the RNA level, it identifies rearrangements/fusions in 45 genes and also quantifies the expression of 2396 cancer-related transcripts. The following histotypes were identified: carcinoma with lymphoid stroma (CLS; 69%), tubular (20%), and mixed (11%). Most cases were associated with atrophic gastritis (71%), and only 11% with dysplasia. The vast majority (94%) of EBVaGCs expressed EBV-encoded RNA in all tumor cells. Mismatch repair deficiency and HER2 overexpression were each observed in 6% of cases, whereas all tumors had a PD-L1-combined positive score $\geq$10. Sixty-six percent of cases showed moderate/strong claudin 18.2 expression in $\geq$75% of cancer cells. The most frequently altered genes were *PIK3CA* (41%) and *ARID1A* (17%). Transcriptomic analysis revealed substantial differential gene expression between EBVaGCs and EBV-negative controls, with upregulation of genes involved in antigen presentation, natural killer cell-mediated cytotoxicity, and cytokine-cytokine receptor interaction in EBVaGCs. Within EBVaGC, CLS showed higher expression of immune-related transcripts and higher PD-L1 expression than other histotypes. This study establishes EBVaGC as a distinct molecular class, with a distinctive profile of genomic alterations and expression of predictive biomarkers, and also with a unique immune microenvironment with enhanced cytotoxic activity. The findings highlight EBV's role in

These authors are cofirst authors: Valentina Angerilli and Jessica Gasparello.
These authors are colast authors: Sara Lonardi and Matteo Fassan.
* Corresponding author.
E-mail address: matteo.fassan@unipd.it (M. Fassan).

https://doi.org/10.1016/j.modpat.2025.100881

early tumor development and EBVaG-CLS as a distinct subgroup within EBVaGC, characterized by unique morphologic features and a pronounced immune activation profile.

Introduction

EBV-associated gastric cancer (EBVaGC) comprises about 1.3% to 30.9% of all gastric cancers (GCs) according to geographic region, with a global average of 8.9% of all GC.[1] EBVaGC tends to have lower mortality rates[2,3] and is preferentially located in the corpus fundus of the stomach.[4] It is associated with a unique histotype, known as carcinoma with lymphoid stroma (CLS), which is characterized by irregular cords, nests, and clusters embedded in a dense lymphocytic infiltrate.[5] Common genetic and epigenetic features of EBVaGC include frequent mutations in *PIK3CA* and *ARID1A*, copy number amplifications of *JAK2* and *CD274*|*PDCD1LG2*, CpG hypermethylation, and *CDKN2A* silencing.[6]

Although EBVaGC represents a distinct morphologic and molecular subtype, the mechanisms of gastric carcinogenesis induced by EBV infection are not yet fully understood. Patients with EBVaGC exhibit unique immune characteristics, including alterations in immune response genes, high PD-L1 expression levels in both cancer and immune cells, increased infiltration of T and natural killer (NK) cells, enhanced expression of immune checkpoint markers, and elevated levels of certain antitumor immunity factors.[7-9]

Recent advancements in GC treatment include immune checkpoint inhibitors like nivolumab and pembrolizumab, approved for use with chemotherapy in advanced or metastatic cases.[10,11] Although patients with PD-L1 expressing tumors benefit from anti-PD-(L)1 treatments, the overall response rates remain modest, typically <20%. However, in EBVaGCs, response rates to these therapies exceed 50%, highlighting EBV positivity as a promising predictive biomarker for treatment efficacy.[12,13]

This study aims to investigate the histopathological and molecular characteristics of a cohort of EBVaGCs, with a particular focus on established prognostic and predictive factors in gastric cancer—such as HER2, mismatch repair (MMR) proteins, PD-L1, and claudin 18.2—complemented by extensive genomic and transcriptomic analyses.

Materials and Methods

Study Cohort

A cohort of 35 patients diagnosed between 2016 and 2022 in 4 large Italian University Hospitals with EBV-associated gastric adenocarcinoma (ie, positive for in situ hybridization [ISH] EBV-encoded RNA [EBER]) were included in this study. Upfront EBER ISH on all GC specimens was performed only in 1 of the participating centers. In the other 3 centers, tumors with morphologic features suggestive of EBV infection (ie, CLS histotype or intense inflammatory infiltrate) were tested for EBER.

Clinical and pathologic data on sex, age, and tumor site were collected from the pathology reports. Medical records were checked for prior *Helicobacter pylori* infection and immunosuppression condition/state. For 3 patients, only biopsy samples were available, whereas in 32 cases, surgical samples were evaluated. In all patients, hematoxylin and eosin-stained slides were jointly reviewed by 2 experienced gastrointestinal pathologists (V.A. and M.F.) to establish pathological Tumor-Node-Metastasis stage (according to the eighth edition American Joint Committee on Cancer staging system criteria[14]), confirm histotype and grade (according to the fifth edition of World Health Organization digestive tumors classification[15]) *H. pylori* status, and investigate additional histologic features, including growth pattern, presence/absence of necrosis, microabscesses, pleomorphism, eosinophils, lymphoid follicles, and eosinophils.

Seven consecutive MMR proficient GCs (ie, nonhypermutated GCs) were selected as controls for transcriptomic analysis.

All information regarding human tissue was managed using anonymous numerical codes, and all samples were handled in compliance with the Declaration of Helsinki. All clinical specimens used in this study were approved by our Institutional Review Board, and were included in the observational retrospective study "GAS-ALL-IN—GAStric cancers a retrospective analysis of ALL major prognostic and predictive determINants."

Tumor-Infiltrating Lymphocytes

Since no standardized guidelines exist for assessing tumor-infiltrating lymphocytes (TiLs) in GC, the international consensus scoring recommendations used for breast cancer were adopted.[16] One representative whole tissue section was selected for evaluation. Specifically, only stromal TiLs were considered, and they were assessed within the tumor borders. Currently, there is no established consensus to define TiL-high or TiL-low in gastric cancer. Therefore, we used a 50% TiL cutoff point, as CLS is typically characterized by high lymphocyte infiltrate.

Epstein-Barr Virus—Encoded RNA In Situ Hybridization

Chromogenic ISH for EBER was performed in formalin-fixed, paraffin-embedded (FFPE) tissue samples with fluorescein-labeled oligonucleotide probes (EBER probe, Ventana) with enzymatic digestion (ISH protease 3, Ventana) and an iViewBlue detection kit (Ventana) with use of the BenchMark ULTRA staining system (K Tello). The average percentage of EBER-positive tumor cells was annotated. EBER ISH was also performed on precursor lesions, if present (ie, dysplasia and atrophic gastritis).

One previously published case with an EBER-positive precursor lesion was included in the cohort.[17] At the time, EBER in situ hybridization was performed using a different protocol (Leica Bond Ready-to-Use EBER probe on the Bond-Max platform). Due to limited remaining tissue, we were unable to repeat EBER staining with the current standardized protocol.

Immunohistochemical Analysis

Immunohistochemical (IHC) stains were performed using the Bond Polymer Refine Detection kit (Leica Biosystems) on BOND-MAX automated IHC Stainer (Leica Biosystems). Four

micrometers thick FFPE sections were incubated with the following primary antibodies according to the laboratory's routine practice: HER2 (4B5, Ventana), PD-L1 (22C3; Dako), p53 (clone DO-7; Dako), claudin 18.2 (CLDN18), (clone 43-14A; Roche Ventana), MLH1 (clone ES05, Dako), PMS2 (clone EP51, Dako), MSH2 (clone FE11, Dako), and MSH6 (clone EP49, Dako).

For the evaluation of HER2, the 4-tiered Hoffmann scoring criteria were used. In surgical specimens, when complete or basolateral membranous reactivity was observed in ≥10% of tumor cells, scores of 1+, 2+, and 3+ were assigned according to the intensity of membranous reactivity (faint, moderate, or intense). In biopsy specimens, when membranous reactivity was observed in at least 1 cancer cell cluster (≥5 cells), scores of 1+, 2+, and 3+ were assigned according to intensity (faint, moderate, or intense).

MMR status was assessed by testing MLH1, PMS2, MSH2, and MSH6, and samples were defined as MMR-deficient (dMMR) when 1 or both proteins from a functional couple resulted negative in the presence of an adequate internal positive control (intratumor inflammatory and stromal cells and nonneoplastic cells).

PD-L1 expression was evaluated by using the combined positive score (CPS) and tumor proportion score (TPS)—CPS = 10, CPS = 50, and TPS = 1% as thresholds. CPS was calculated by dividing the number of PD-L1-positive cells (tumor, lymphocytes, and macrophages) by the total number of viable tumor cells, then multiplying by 100. PD-L1 expression was evaluated on whole slides, evaluating multiple representative regions/multiple fields.[18,19] TPS was determined by dividing the number of PD-L1-positive tumor cells by the total number of viable tumor cells, then multiplying by 100 and reporting the value as a percentage.[18,19]

p53 immunophenotype was considered "mutant" in the presence of complete loss or diffuse and strong nuclear immunostaining in neoplastic cells.

CLDN18 immunoreactivity was evaluated with a quantitative (percentage of stained tumor cells) method. Tumors with a 2+/3+ score of CLDN18 intensity in ≥75% of tumor cells, which is the IHC cutoff being used for eligibility in ongoing zolbetuximab clinical trials, were considered positive for CLDN18.[20]

Nucleic Acids Isolation

Ten 5-μm sections were obtained from the respective FFPE block. Following the pathologist's selection, an equal number of sections (5) were manually macrodissected for the isolation of both DNA and RNA. After the dewaxing of paraffin sections, DNA and RNA were extracted using QIAmp FFPE tissue kit (Qiagen) and RNeasy FFPE kit (Qiagen), respectively, according to the manufacturer's instructions. Both nucleic acids were then quantified using Qubit 4.0 (Thermo Fisher Scientific) fluorometer and its assays: Qubit DNA HS Assay kit (Thermo Fisher Scientific) and Qubit RNA HS Assay kit (Thermo Fisher Scientific) for DNA and RNA, respectively.

MLH1 Promoter Methylation Assay

The p*MLH1* methylation analysis was performed on samples that were determined to be dMMR, with loss of MLH1/PMS2, at IHC, and was determined following the *MGMT* Plus protocol instructions (Diatech Pharmacogenetics). Bisulfite conversion was performed after sample quantification with the spectrophotometer DropSenseTM 16 (Diatech Pharmacogenetics). The converted DNA was amplified with Rotor-Gene 6000 (Corbett Research, Qiagen) and subsequently sequenced with PyroMark Q96 ID (Qiagen) using pyrosequencing technology. Samples were defined as not methylated if the methylation rate was <5%, undetermined if between ≥5% and <10%, and methylated if it was ≥10%.[21]

Molecular Profiling With AmoyDx Master Panel

Genomic and transcriptomic characterization was performed using the AmoyDx Master Panel (Amoy Diagnostics), a comprehensive genomic profiling panel encompassing 571 genes. Regarding DNA, in addition to single-nucleotide variants/indel, fusion, and copy number variations (CNVs) analysis, the panel also evaluates complex signatures including homologous recombination deficiency (HRD), microsatellite instability (MSI), and tumor molecular burden (TMB). At the RNA level, the panel analyses >2000 transcripts, detecting fusions and alternative splicing, quantifying gene expression (gene expression profiling) of genes implicated in cancer pathways and immune response, and defining the tumor microenvironment (TME). The panel can also detect EBV transcripts, including EBER1, EBER2, BARF1, LMP2A, EBNA1, and BZLF. According to the manufacturer's protocol, 150 ng of genomic DNA and 200 ng of total RNA were enzymatically fragmented using KAPA Frag kit (KK8602, Roche). Fragmented nucleic acids were purified using AMPure XP beads (Beckman Coulter) and employed for the preparation of next-generation sequencing (NGS) libraries. Qubit dsDNA HS Assay kit (Thermo Fisher Scientific) was used to quantify the hybridization capture-enriched NGS libraries, whereas High Sensitivity DNA ScreenTape Analysis Reagents and TapeStation 4200 System (Agilent Technologies) were used to assess the size of the obtained library's fragments. NGS sequencing was performed on a NextSeq 550Dx instrument (Illumina) using a NextSeq 500/550 HighOutput v2.5 (300 cycles) kit.

Molecular Profiling: Bioinformatic Analysis

Raw base-call data generated by the Illumina NextSeq 550Dx system were demultiplexed, converted to FASTQ format, and analyzed with the AmoyDx NGS data analysis system (ANDAS). The manufacturer's quality control criteria were used to determine whether the result was valid, including median insert size ≥150 bp, the percentage of target region covered (coverage) ≥95%, and the proportion of reads mapping to the target region (readsOnTarget) ≥60%. According to the AmoyDx Master Panel analysis guidelines, high TMB was defined for more than 7.76 mutations per megabase (mut/Mb), whereas MSI was defined for ≥15% of microsatellite unstable sites. The genomic instability status was defined by calculating the genomic scar score, using AmoyDx's proprietary algorithm, based on the analysis of 19 genes involved in the homologous recombination mechanism. A cutoff value of ≥50 was set by the manufacturer to define the sample as positive for the HRD. Genetic alterations (single-nucleotide variants, insertion/deletion: Indels) were classified according to the TIER classification by searching in Franklin by Genoox, ClinVar, and cBioPortal databases. Gene rearrangements and splice variants are detected in RNA. According to gene expression profiling, samples were classified by ANDAS software into 4 different subtypes: immune-enriched, fibrotic, immune-enriched, nonfibrotic, fibrotic, and desert. Positivity to EBV infection was calculated based on the sum of EBER1 and EBER2 FPKM (fragments per kilobase of exon model per million mapped fragments). Gene expression profiling analysis was evaluated for 2396 transcripts, starting from raw counts that were normalized

and analyzed using DESeq2 1.26.0 Bioconductor package within the R version 4.2.1 (R Core Team). Similarities between samples were investigated using unsupervised hierarchical clustering and principal component analysis. Differentially expressed transcripts were identified, and transcripts presenting a $Log_2FC \geq 1.5$ or ≤ -1 ($P < .05$) were considered up- or down-regulated, respectively. Differentially expressed genes (DEGs) were imported into the STRING database (version 12) and analyzed to identify protein-protein interaction networks, setting a confidence level >0.4, and functional enrichment analyses. For functional enrichment analyses, Kyoto encyclopedia of genes and genomes (KEGG) and Reactome pathway analysis were performed, setting the threshold at $P < .05$. Normalized expression of the 2396 sequenced transcripts was employed to identify differences in immune cell subtype abundance among the analyzed cases. Transcriptomically profiled cases were analyzed using Consensus^{TME} (olliecast.shinyapps.io/Deconvolution_Benchmarking/), obtaining as output normalized enrichment scores (NES), able to capture the relative level of estimated abundance of specific cell types across samples.

Statistics

The Mann-Whitney *U*-test was used to compare the distributions of NES value for each immune cell type. Statistical differences were considered significant when $P < .05$. Statistical analyses were carried out using GraphPad Prism version 5.

Results

Clinicopathologic Features and Epstein-Barr Virus-Encoded RNA In Situ Hybridization

Most patients were male (66%) and >65 years at diagnosis (60%). The most frequent site was the corpus fundus of the stomach (49%). Two cases developed at the anastomotic site of a previous partial gastrectomy performed 40 and 32 years earlier, respectively. In both instances, the initial surgery had been carried out for a benign gastric ulcer. The vast majority of the tumors were pT3-pT4 (72%); lymph node involvement was observed in 53% of cases. As for histotype, most EBVaGC (69%) were CLS, followed by tubular adenocarcinomas (20%) and mixed-type carcinomas (ie, composed of a tubular and a poorly cohesive component; 11%). Among the 21 cases that were selected by EBV upfront testing, 12 were CLS (57%), 7 were tubular (33%), and 2 were mixed (10%). Overall, 69% of EBVaGC showed vascular invasion, whereas 17% showed perineural invasion. As for associated precursor lesions, 71% of cases were associated with metaplastic atrophic gastritis, and 11% (4 cases) were associated with both metaplastic atrophic gastritis and dysplasia. No patient had a background of autoimmune gastritis with loss of parietal cells. *H. pylori* infection was documented in 5 cases (14%). Four of 5 patients with *H. pylori* infection had metaplastic atrophic gastritis. No previously documented *H. pylori* infection was reported. There was no record of immunosuppression in any patient.

Representative images of hematoxylin and eosin and EBER-stained slides of various histotypes of EBVaGCs are shown in Figure 1.

The detailed clinicopathologic features of all 35 EBVaGC cases included in the study are reported in Table 1.

When characterizing the morphologic heterogeneity of EBV-associated CLS (EBVaGCLS; n = 24), we observed that syncytial growth was the most frequent growth pattern (71%), followed by solid (13%), trabecular (8%), and mixed trabecular glandular (8%). Most cases had nuclear pleomorphism (63%), whereas only a minor part had tumor necrosis (17%). As for tumor-associated inflammatory infiltrate, microabscesses were found in 42% of EBVaGCLS, eosinophils in 46%, and lymphoid follicles in 20% (Supplementary Fig. S1A-C).

EBER was expressed in 90% to 100% of tumor cells in the vast majority of the samples (94%). It was expressed in 5% of tumor cells in 1 CLS, and in 1 mixed EBVaGC, EBER was expressed in 60% of tumor cells.

All precursor lesions (ie, atrophic gastritis and dysplasia) were EBER-negative (Supplementary Fig. S1D, E), except for 1 case of foveolar dysplasia associated with a tubular low-grade EBVaGC. Atrophic metaplastic gastritis was also present in this case, but it was EBER-negative. The case was described in detail in a previous publication by our group.[17] Of note, 1 CLS case had adjacent EBER-positive normal mucosa (Supplementary Fig. S1F).

Evaluation of Tumor-Infiltrating Lymphocytes and Immunohistochemical Analysis

High TiLs were observed in 49% of EBVaGC and were more frequent among CLS ($P = .0027$). Only 2 cases of EBVaGC were dMMR (both CLS), showing loss of the heterodimer MLH1/PMS2. The methylation assay demonstrated that both dMMR EBVaGC were methylated in p*MLH1*. One of the 2 dMMR CLS showed EBER expression in 5% of tumor cells, whereas the other had EBER expression in 100% of tumor cells.

PD-L1 was highly expressed (CPS ≥10) in all EBVaGC, but very high CPS values (CPS ≥50) were observed more frequently in CLS ($P = .0271$). As for PD-L1 expression in tumor cells, 54% of EBVaGC were TPS ≥1%, with CLS more frequently exhibiting TPS ≥1% ($P = .0088$). The majority of HER2 was overexpressed in 2 tubular EBVaGC (6% of EBVaGC), whereas CLDN18 was positive in the majority of cases (66%); no difference in CLDN18 positivity was observed between CLS and other histotypes. p53 expression was mutant in 20% of EBVaGC.

Evaluation of TiLs and IHC features is reported in Table 2. Representative examples of EBVaGCLS and IHC stains are shown in Figure 2.

Genomic Profiling

Molecular analysis was performed in 29 samples because 6 samples were excluded due to low nucleic acid quantity/quality.

The analysis of single-nucleotide variants, insertions and deletions variants, and CNVs, revealed a total of 62 genetic alterations affecting 39 different genes with a range of 0 to 17 variants per sample after excluding synonymous, intronic variants, high-incidence polymorphisms in the population, and benign/likely benign alterations (Supplementary Fig. S2).

Nonsynonymous coding variants were the most common genetic alterations (55%), followed by frameshift deletions/insertions (31%) and CNVs (14%).

PIK3CA and *ARID1A* mutations were the most frequent in the cohort (41% and 17% of cases, respectively), followed by *CTNNB1* (10%). *KTM2D*, *APC*, *CCND1*, *FGFR2,* and *KMT2C* GAs were all detected in 2 samples each (7%). No differences in the frequency of *PIK3CA* and *ARID1A* mutations were observed among the histotypes.

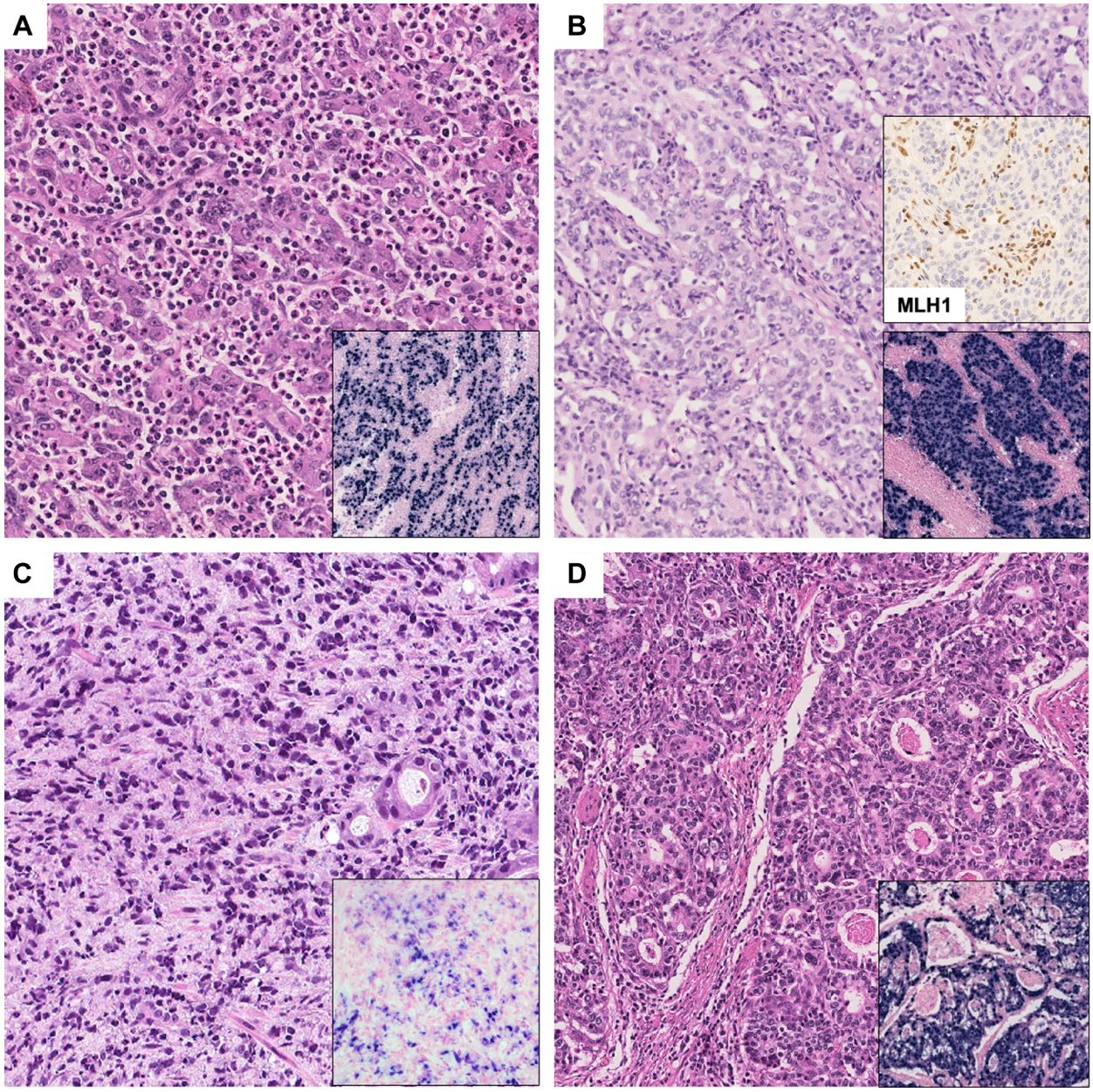

Figure 1.
Representative images of Epstein-Barr virus (EBV)-associated gastric carcinomas with inlet EBV-encoded RNA (EBER)-positive staining. (A) Gastric carcinoma with lymphoid stroma (CLS) with lymphoepithelioma-like features; (B) gastric CLS with medullary-like features with MLH1/PMS2 immunohistochemical loss (inlet MLH1 staining); (C) mixed-type gastric carcinoma (only poorly cohesive component shown); and (D) high-grade tubular adenocarcinoma.

PIK3CA mutations were located in different exons, including exons 20, 9, 4, 2, and 14. The most frequent *PIK3CA* mutation was the missense E545K (3/12); 2 cases harbored a double *PIK3CA* mutation.

CNVs, including the amplification of *CCND1* (7%), *KMT2D*, *FGFR2*, *CD274*, *FGF19*, *FGF3*, *MDM2*, and *MYC* (4% each) genes, were found.

MSI status was observed in the 2 samples that were labeled as dMMR at IHC. TMB high was found in 21% of samples, encompassing one of the 2 dMMR/MSI EBVaGC. None of the EBVaGC analyzed samples presented a positive genomic scar score, indicating that none of them presented HRD.

Figure 3 summarizes the clinicopathologic features, biomarker status, and genetic alterations of 35 EBVaGCs.

Transcriptomic Analysis

Gene Expression Profiling of Epstein-Barr Virus-Associated Gastric Cancer vs Nonhypermutated Epstein-Barr Virus—Negative Gastric Cancer Controls

To identify the DEGs between 29 EBVaGCs and 7 non-hypermutated EBV-negative controls, a supervised approach was used (Fig. 4; Supplementary Fig. S3A). As a result, we obtained a total of 214 DE genes, of which 71 were upregulated and 143 were downregulated in EBVaGC. Based on fold change values, the 10 most upregulated genes in EBVaGC were: *EBER2*, *EBER1*, *BARF1*, *LMP2A*, *CD160*, *GZMH*, *CXCL11*, *CD244*, *GZMA*, and *CXCK9*, whereas the 10 most downregulated genes were *KRT13*, *KRT14*, *KRT6C*, *KRT5*, *PPP2R2C*, *S100A2*, *CALML3*, *KRT6A*, *KRT15*, and *SERPINB3*. Of

Table 1
Clinicopathologic features of 35 Epstein-Barr virus–associated gastric adenocarcinomas

Clinicopathologic feature	Number of cases
Sex	
M	23 (66%)
F	12 (34%)
Age (y)	
<65	14 (40%)
≥65	21 (60%)
Site	
Cardias	5 (14%)
Corpus/fundus	17 (49%)
Antrum/angulus	11 (31%)
Anastomosis	2 (6%)
pT[a]	
pT1	3 (9%)
pT2	6 (19%)
pT3	16 (50%)
pT4	7 (22%)
pN[a]	
pN0	15 (47%)
pN1	7 (22%)
pN2	6 (19%)
pN3	4 (12%)
Histotype	
Carcinoma with lymphoid stroma	24 (69%)
Tubular	7 (20%)
- *Low-grade*	- *1*
- *High-grade*	- *6*
Mixed	4 (11%)
Lymphovascular invasion	
Present	24 (69%)
Absent	11 (31%)
Perineural invasion	
Present	6 (17%)
Absent	29 (83%)
Helicobacter pylori status	
Positive	5 (14%)
Negative	30 (86%)
Atrophic gastritis	
Present	22 (71%)
Absent	9 (29%)
Dysplasia	
Present	4 (11%)
Absent	31 (89%)

F, female; M, male.
[a] Information not available for 3 cases.

note, the 4 most upregulated genes, as expected, are all EBV-related transcripts (*EBER2*, *EBER1*, *BARF1*, and *LMP2A*). The EBV-related transcripts *EBNA1* and *BZLF1* were also found to be upregulated in EBVaGC, without, however, reaching statistical significance. Among checkpoint regulator genes, we found *IDO1*, *LAG3*, *CD96*, *CTLA4,* and *TIGIT* to be upregulated in EBVaGCs, with fold changes ranging from 7 to 2.2. The CD274 (PD-L1) and PDCD1 (PD-1) transcripts were also found to be modulated, although not statistically significant, in our data set. Out of 95 chemokine/cytokine-encoding genes, the proinflammatory cytokine CXCL10 and the cytokines CXCL11 and CXCL9 were all found to be upregulated in EBVaGCs, together with their interacting receptor, CXCR3. In the same subgroup, the inflammatory cytokine CCL4 and its binding receptor CCR5, interacting with several inflammatory chemokines, were reported as upregulated, whereas CXCL14, a potent chemoattractant for neutrophils, but not for T- and B-cells, was downregulated. A total of 48 cancer-related genes were found to be DE, 11 were upregulated, and 37 were downregulated in EBVaGCs. Among the 11 upregulated cancer-related transcripts, 5 encode immune-related proteins, including *IL21R*, *TAP1*, *B2M*, and the transcription factor STAT1. STAT1 is a key component of the Janus kinase-STAT signaling pathway and plays a central role in regulating the expression of numerous immune-related genes. One of these is interferon regulatory factor 1, which was also found to be upregulated in this group. The 2 most downregulated cancer-related genes by fold change value encompass genes inducing the basal-like/squamous subtype (*SERPIN3B*, *TP63)*. Other notable downregulated oncogenes include *RET*, *EGFR,* and *MYCN.* Pathway enrichment analysis was performed using KEGG and Reactome databases to identify significantly overrepresented pathways. The KEGG pathway enrichment analysis highlighted several key signaling pathways implicated in cellular processes, including the PI3K-Akt and MAPK signaling pathways, which play crucial roles in cell proliferation, survival, and differentiation. Other significantly enriched pathways included those involved in cytokine-cytokine receptor interactions, TGF-β signaling, and pathways associated with cancer progression and stem cell pluripotency regulation. Similarly, the Reactome pathway enrichment analysis identified immune-related processes as significantly enriched, with pathways such as antigen processing and presentation, adaptive immune system responses, and T-cell receptor (TCR) signaling being prominently represented. Additionally, pathways related to extracellular matrix organization and signal transduction underscore the importance of cell-cell and cell-matrix interactions in the biological system under investigation.

Gene Expression Profiling of Epstein-Barr Virus–Associated Carcinoma With Lymphoid Stroma vs Epstein-Barr Virus–Associated Gastric Cancer of Other Histotypes

To identify the DE genes between 21 EBVaGCLS and 8 EBVaGCs presenting other histotypes, a supervised approach was used (Fig. 5; Supplementary Fig. S3B). As a result, we identified 72 DE genes in EBVaGCLS, with 58 upregulated and 14 downregulated. Among the most upregulated transcripts, based on fold change values, were genes encoding the chemotactic factor CCL18 (which attracts naïve, CD4+, and CD8+ T cells), GNLY, ZBTB32, HLA-G, CXCR6, GZMH, the cytokine CXCL9 and its receptor CXCR3, NKG7, and IDO1, a known suppressor of antitumor immune responses. The 5 most downregulated genes were *APOA2*, *HBB*, *C7*, *PRSS1*, and *LAMC3*. Additionally, several key regulators of the Wnt signaling pathway—*AXIN2*, *RNF43*, *PTK7*, and *SFRP1*—were also downregulated. *BAMBI*, a negative regulator of TGF-β signaling, was likewise found to be downregulated. No DE EBV-related transcript was found between the 2 groups. Among checkpoint regulators, IDO1 and PDCD1 (PD-1) transcripts were found to be upregulated in EBVaGCLS. A total of 15 cancer-related genes were found to be DE, 8 were upregulated (*PDCD1*, *ITK*, *IL21R*, *RAC2*, *LCK*, *IKZF1*, *PIK3CD*, and *CD74*), and 7 were downregulated in EBVaGCLS (*AXIN2*, *PRSS1*, *RNF43*, *SFRP1*, *PTK7*, *ERBB2,* and *GRB7).* Notably, the downregulated gene *GRB7* is involved in the activation of key downstream protein kinases, including STAT3, AKT1, MAPK1, and MAPK3, as well as in the activation of HRAS. The KEGG pathway enrichment analysis revealed significant activation of immune-related pathways, including Th1 and Th2 cell differentiation, Th17 cell differentiation, and antigen processing and presentation, suggesting a strong involvement of adaptive immunity. Notably, pathways associated with allograft rejection, graft-versus-host disease, and autoimmune disorders such as type 1 diabetes mellitus and autoimmune thyroid disease were also enriched, indicating a potential dysregulation of immune

Table 2
Evaluation of tumor-infiltrating lymphocytes and immunohistochemical features of 35 Epstein-Barr virus–associated gastric adenocarcinomas

Histopathological and molecular feature	EBVaGC (n = 35)	CLS (n = 24)	Tubular/mixed (n = 11)	*P* value
Tumor-infiltrating lymphocytes				
High	17 (49%)	16 (67%)	1 (9%)	.0027
Low	18 (51%)	8 (33%)	10 (91%)	
EBER				
<25%	1 (3%)	1 (4%)	0 (0%)	.5361
25%-75%	1 (3%)	0 (0%)	1 (9%)	
>75%	33 (94%)	23 (96%)	10 (91%)	
MMR proteins				
dMMR	2 (6%)	2 (8%)	0 (0%)	1.000
MMRp	33 (94%)	22 (92%)	11 (100%)	
PD-L1 (CPS)				
CPS<10	0 (0%)	0 (0%)	0 (0%)	.0271
10≤CPS≤50	15 (43%)	7 (29%)	8 (73%)	
CPS>50	20 (57%)	17 (71%)	3 (27%)	
PD-L1 (TPS)				
TPS<1%	16 (46%)	7 (29%)	9 (82%)	.0088
TPS≥1%	19 (54%)	17 (71%)	2 (18%)	
HER2				
Overexpressed	2 (6%)	0 (0%)	2 (18%)	.0924
Not overexpressed	33 (94%)	24 (100%)	9 (82%)	
CLDN18				
Positive	23 (66%)	18 (75%)	5 (45%)	.1297
Negative	12 (34%)	6 (25%)	6 (55%)	
p53				
Mutant	7 (20%)	4 (20%)	3 (27%)	.6524
Wild-type	28 (80%)	20 (80%)	8 (73%)	

CLS, carcinoma with lymphoid stroma; CPS, combined positive score; dMMR, deficient MMR; EBVaGC, Epstein-Barr virus–associated gastric cancer; MMR, mismatch repair; TPS, tumor proportion score.

tolerance mechanisms. The Reactome pathway enrichment analysis further reinforced this immunological focus, highlighting key pathways such as PD-1 signaling, TCR signaling, and downstream TCR signaling events. Additionally, pathways related to immunoregulatory interactions between lymphoid and non-lymphoid cells, as well as chemokine receptor binding, suggest an intricate network of immune modulation.

Using a set of 2396 transcripts quantified in both EBVaGC and nonhypermutated EBV-negative GC, the cell type enrichment of the TME has been studied, producing NESs used to identify differences in immune cell subtype abundance between analyzed cases. High heterogeneity among analyzed samples was reported, although a trend toward clustering of the 2 subgroups is appreciable (Supplementary Fig. S4). A significant increase of both

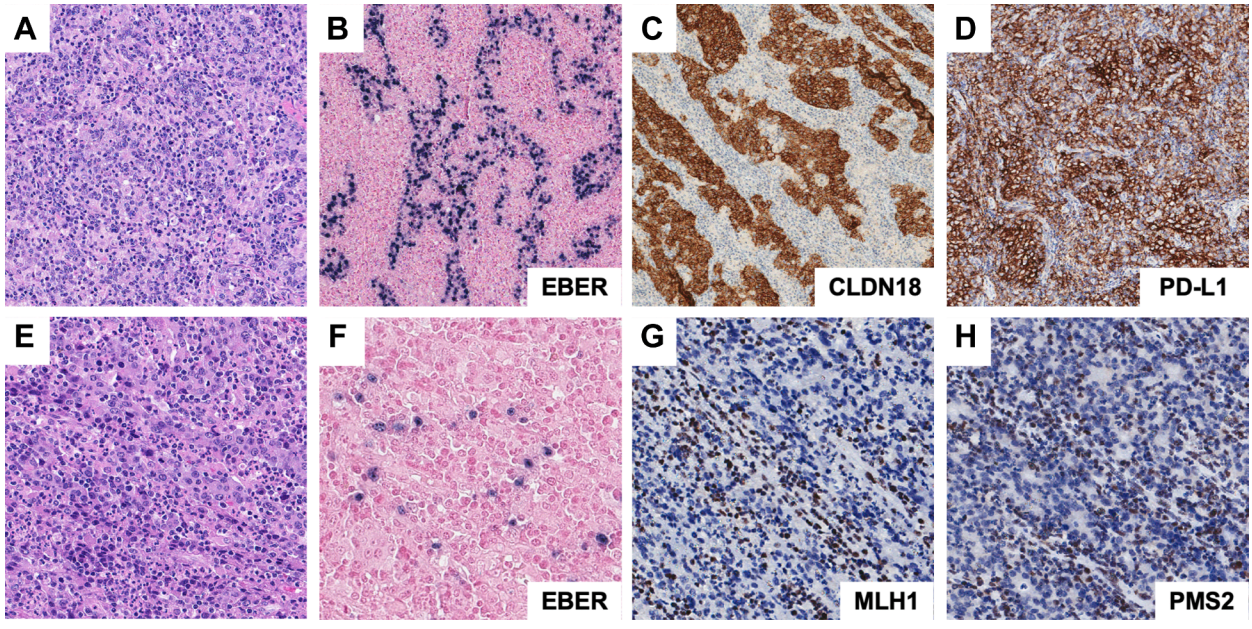

Figure 2.
(A) Gastric carcinoma with lymphoid stroma (CLS) showing (B) diffuse Epstein-Barr virus (EBV)-encoded RNA (EBER) positivity (C) CLDN18 positivity and (D) PD-L1 combined positive score of 100. (E) Gastric CLS showing (F) EBER positivity in 5% of tumor cells and (G) MLH1 and (H) PMS2 loss.

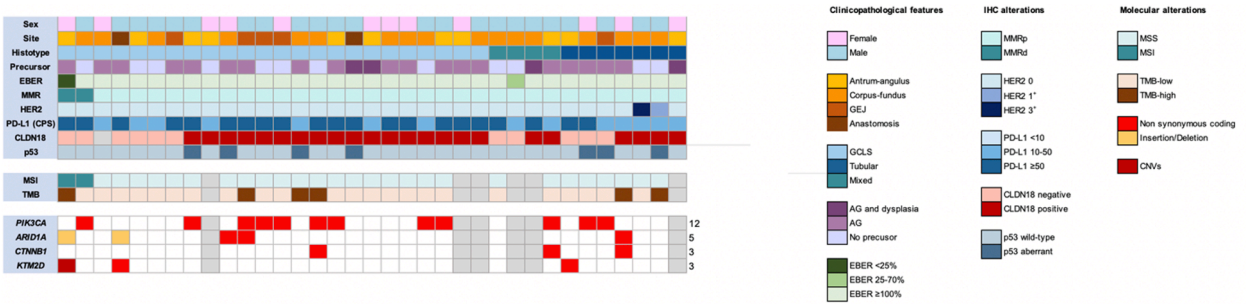

Figure 3.
Summary of clinicopathologic features, biomarker status, and genetic alterations of 35 Epstein-Barr virus (EBV)-associated gastric carcinomas, of which 29 underwent extensive molecular profiling. AG, atrophic gastritis; CLDN18: Claudin 18; CNVs, copy number variations; CPS, combined positive score; EBER, EBV-encoded RNA; GCLS, gastric carcinoma with lymphoid stroma; GEJ, gastroesophageal junction cancer; IHC, immunohistochemical; MMR, mismatch repair proteins; MSI, microsatellite Instability.

CD8+ (panel a) and CD4+ (panel b) T cells was reported in EBVaGCs, which also presented an increase in eosinophil, neutrophil, and monocyte (panels h, k, and n) content in the TME.

Discussion

EBVaGCs comprise 5% to 10% of GCs worldwide and are pathologically, molecularly, and immunologically distinct entities from EBV-negative GCs.[22] Because the majority of EBVaGCs are PD-L1-expressing tumors, current international guidelines do not include EBV status as a predictive biomarker in the metastatic setting.[10,11] However, EBVaGCs are reported to have a much higher response rate to anti-PD-1 therapy than EBV-negative GCs,[23] and several clinical trials are currently underway to evaluate the efficacy of various immune checkpoint inhibitors targeting the PD-1/PD-L1 axis specifically in EBVaGC. Additionally, other immunotherapeutic approaches, such as CAR-T cells, CAR-NK cells, and cancer vaccines, are currently being explored as potential treatment options for EBVaGC.[24-26] Thus, it is crucial to

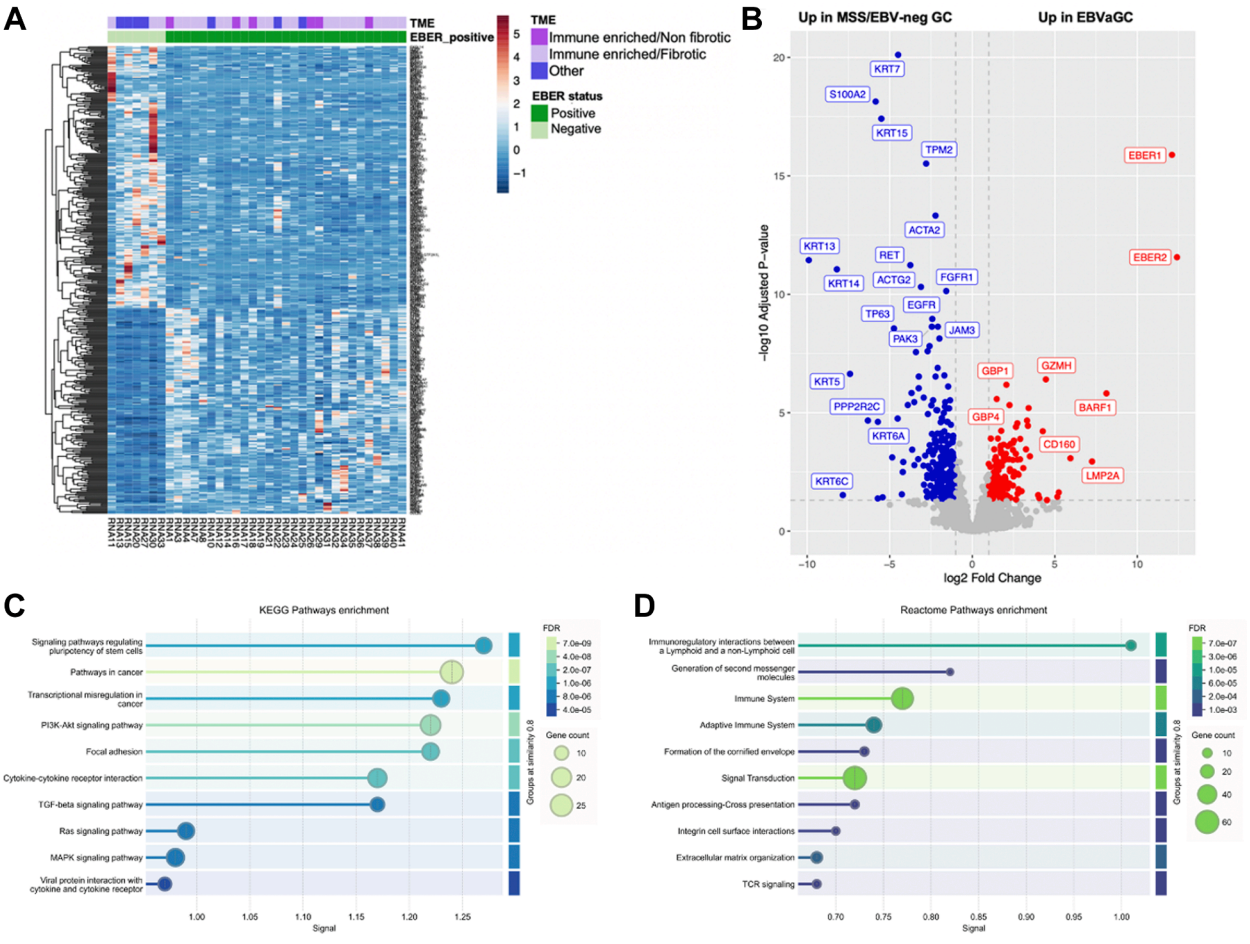

Figure 4.
(A) Heatmap reporting the top 500 deregulated transcripts and (B) Volcano plot showing differentially expressed genes between 29 EBVaGC and 7 MSS/EBV-negative EBV-negative controls (Log2FC ≥1.5 or ≤−1). Pathway enrichment plots using (C) KEGG and (D) Reactome database. EBER, EBV-encoded RNA; EBV, Epstein-Barr virus; EBVaGC, EBV-associated gastric carcinoma; KEGG, Kyoto encyclopedia of genes and genomes; MSS, microsatellite instable; TME, tumor microenvironment.

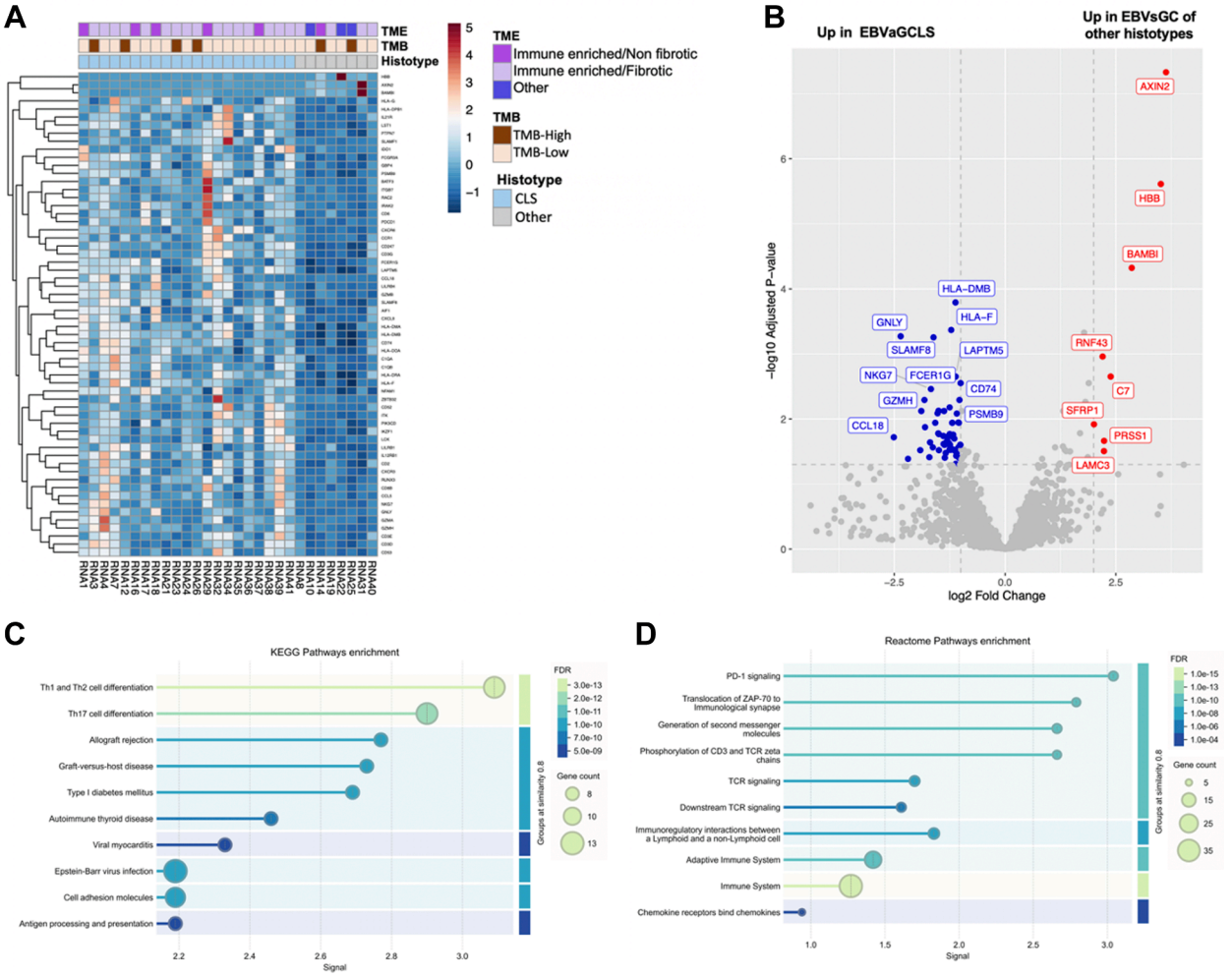

Figure 5.
(A) Heatmap reporting the most 60 upregulated transcripts among the 2 subtypes (EBVaGCLS vs EBVaGC of other histotypes) and (B) Volcano plot showing differentially expressed genes ($Log_2FC>2$; Log2FC<-1) between 21 EBVaGCLS and 8 EBVaGC of other histotypes. Pathway enrichment plots using (C) KEGG and (D) Reactome database. CLS, carcinoma with lymphoid stroma; EBV, Epstein-Barr virus; EBVaGCLS, EBV-associated gastric carcinoma with lymphoid stroma; EBVaGC, EBV-associated gastric carcinoma; KEGG, Kyoto encyclopedia of genes and genomes; TMB, tumor molecular burden.

better understand the pathogenesis, the molecular and immunological landscape of EBVaGC, and its association with other clinically relevant biomarkers.

In this retrospective study, we analyzed a series of EBVaGCs to investigate their clinicopathological, morphological, and molecular characteristics. Consistent with previous findings,[5] we observed a predominance of male patients and proximally located tumors, and a significant proportion of patients were <65 years old. EBVaGC exhibited a preponderance of CLS and showed high levels of TiLs regardless of histologic subtype. In agreement with The Cancer Genome Atlas Program (TCGA) data,[27] our cohort of EBVaGC was enriched in mutations in the *PI3KCA* gene, located in various exons, and *ARID1A* had infrequent *TP53* mutations. However, we found lower rates of *PI3KCA* and *ARID1A* mutations and no *JAK2* or *ERBB2* amplification than in TCGA data.[27] Transcriptomic analysis revealed a high degree of homogeneity in EBVaGC, reflected by the substantial number of DEGs identified between EBVaGC and controls. EBVaGCs showed a remarkable overexpression in genes encoding for chemokines and chemokine receptors of the CC and CCX subfamilies, interleukin, and interleukin receptors. Genes related to NK cell-mediated cytotoxicity were markedly overexpressed in EBVaGCs, including genes expressed on the surface of NK cells (*CD160*, *CD244*, *CD226*, and *CD96*), genes encoding for granzymes (*GZMH*, *GZMA*, and *GXMB*), and genes promoting NK cell cytotoxicity (*KLRK1*, *CRTAM*, *CD84*, *NKG7*, *GNLY*, and *LAG3*). Several genes involved in antigen processing and presentation were also upregulated, especially those involved in the MHC-I pathway, promoting CD8-positive T-cell and NK cell cytotoxicity, such as B2M, HLA-A, and HLA-F. It is important to note that <2400 transcripts have been quantified; therefore, additional molecular pathways are likely to be affected if the entire transcriptome is analyzed.

The EBVaGC cohort analyzed in this study revealed a unique profile of biomarker expression. All samples exhibited high levels of PD-L1 expression (CPS $\geq$10), and the majority showed PD-L1 expression in tumor cells (TPS $\geq$1%). A recent meta-analysis of 43 studies, including a total of 11,327 patients, demonstrated a strong association between PD-L1 expression and EBVaGC, with an odds ratio of 6.36 (95% CI: 3.91-10.3, $P < .001$).[12] The mechanisms behind this elevated PD-L1 expression are still unclear; a

previous study has shown that the increase in PD-L1 likely occurs as a response to higher levels of IFN-γ via activation of IRF3.[28] In this study, no upregulated transcripts of the IRF3 pathway were identified; however, upregulated transcripts of the IFN-γ Janus kinase/STAT pathway, including STAT1 and interferon regulatory factor 1, were observed. Of note, other potentially targetable checkpoint regulator genes we found to be upregulated in EBVaGCs include *IDO1*, *LAG3*, *CD96*, *CTLA4*, and *TIGIT*. CLDN18 was positive in 66% of EBVaGCs. This prevalence is consistent with previous translational studies.[29-31] Our findings indicate that the overlap between EBV infection and HER2 overexpression or dMMR is rare, but possible. The co-occurrence of EBV infection and HER2 overexpression has been previously documented,[32] whereas the overlap between EBV infection and dMMR is still controversial. According to TCGA molecular classification of GC,[27] p*MLH1* methylation and EBV infection are mutually exclusive, with EBVaGCs showing methylation of p*CDKN2A*.[33] In contrast, a previous report by Martinez-Ciarpaglini et al[34] reported the coexistence of EBV infection by ISH and MSI/dMMR in 3 cases. Consistent with our findings, Martinez-Ciarpaglini et al[34] observed EBER expression in a minor fraction of tumor cells in 2 of the 3 cases.

The results of this study provide valuable insights into the pathogenesis of EBVaGC. First, atrophic gastritis was observed in a significant number of cases, suggesting that EBV-associated carcinogenesis may develop in gastric mucosa that has undergone morphologic and molecular changes, reaching the so-called "point of no return" as a consequence of *H. pylori* infection, often resolved and undocumented, or other harmful conditions (eg, bile reflux).[35] Second, in the vast majority of cases, EBER expression was detected in the vast majority of tumor cells. The clonality of the EBV genome within tumor cells suggests that the virus plays a role in the early stages of carcinogenesis. Fukayama et al[36] propose that gastric mucosal cells infected by EBV may undergo malignant transformation, leading to the clonal expansion of these transformed epithelial cells and the progression toward cancer. The finding of 1 EBER-positive dysplasia and EBER-positive normal gastric mucosa corroborates this hypothesis. As for the carcinogenic cascade of CLS, (1) the absence of EBER-positive dysplasia associated with CLS, (2) the consistent EBER expression across all tumor cells in CLS, and (3) the presence of EBER-positive gastric mucosa adjacent to 1 CLS suggest that EBVaGCLS may not arise from dysplasia as a precursor lesion. Instead, the dysplastic lesions identified in the 2 cases of EBVaGCLS were linked to atrophic gastritis and may have developed as part of a cancerization field, representing a distinct clone unrelated to EBV infection.[35]

A growing body of evidence has established EBVaGC as a distinct class of GC. Our findings suggest that EBVaGCLS represents a distinct subgroup within EBVaGC with peculiar morphologic characteristics closely reflected in its underlying biology. EBVaGCLS harbor marked upregulation of immune and inflammatory genes and pathways, including those encoding cytokines, cytokine receptors, genes related to NK cell-mediated cytotoxicity, and genes involved in antigen processing and presentation. This upregulation is associated with enhanced lymphocytic infiltration and higher levels of PD-L1 expression in comparison to EBVaGCs of other histotypes. Moreover, the reconstruction of TME from the transcriptomic profile detected in the neoplasms reveals that EBVaGCLS appear to be enriched in T cells, particularly $CD8^+$ ones. From a morphologic standpoint, we observed a certain degree of heterogeneity within the EBVaGCLS subgroup in terms of architecture, composition of the inflammatory infiltrate, and the level of atypia. Thus, a clear distinction between medullary carcinoma and lymphoepithelioma-like carcinoma could not be made. This finding further supports the notion that CLS should be categorized based on integrating EBV and/or MSI association, rather than subtyped based on histologic features only.

To conclude, this study establishes EBVaGC as a distinct molecular class, with a distinctive profile of genomic alterations and expression of predictive biomarkers and with a specific immune microenvironment with high immune gene expression and enhanced cytotoxic activity. These findings highlight EBV's role in early tumor development and EBVaGCLS as a distinct subgroup within EBVaGC, characterized by unique morphological features and a pronounced immune activation profile.

Author Contributions

V.A., J.G., and M.F. performed study concept and design; V.A., J. G., F.G., and P.P. performed development of methodology and writing, A.V., A.P.D.T, L.M., R.G., F.B., C.L., S.L., and M.F. review and revision of the paper; J.G., A.C., C.C., and M.S. provided acquisition, analysis and interpretation of data, and statistical analysis; C.C., J.G., M.N., and M.S. provided technical and material support. All authors read and approved the final paper.

Data Availability

The data that support the findings of this study are available from the corresponding author upon reasonable request.

Funding

M.F. is supported by BIRD-2024 (FASS_BIRD24_01) funds from the Department of Medicine (DIMED), University of Padua. This work has been also funded by the European Union (EU)—Next-Generation EU ("PNRR M4C2-Investimento 1.4-CN00000041").

Declaration of Competing Interest

None reported.

Ethics Approval and Consent to Participate

All clinical specimens used in this study were approved by our Institutional Review Board, and was included in the observational retrospective study "GAS-ALL-IN—GAStric cancers a retrospective analysis of ALL major prognostic and predictive determINants." The study was performed according to the clinical standards of the 1975 and 1983 Declaration of Helsinki.

Declaration of Generative AI and AI-Assisted Technologies in the Writing Process

During the preparation of this work the author(s) used no generative AI tools in the conception, execution, analysis, or writing of this study.

Supplementary Material

The online version contains supplementary material available at https://doi.org/10.1016/j.modpat.2025.100881.

References

1. Yang J, Liu Z, Zeng B, Hu G, Gan R. Epstein-Barr virus-associated gastric cancer: a distinct subtype. *Cancer Lett*. 2020;495:191–199. https://doi.org/10.1016/j.canlet.2020.09.019
2. Chen X, Chen S, Wang X, et al. Analysis and external validation of a nomogram to predict peritoneal dissemination in gastric cancer. *Chin J Cancer Res*. 2020;32(2):197–207. https://doi.org/10.21147/j.issn.1000-9604.2020.02.07
3. Ying T, Chen J, Song J, Zhou Y, Bao B, Zheng L. Prognosis of EBV-positive gastric cancer with lymphoid stroma: systematic review and meta-analysis. *Scand J Gastroenterol*. 2024;59(3):316–324. https://doi.org/10.1080/00365521.2023.2286194
4. Camargo MC, Murphy G, Koriyama C, et al. Determinants of Epstein-Barr virus-positive gastric cancer: an international pooled analysis. *Br J Cancer*. 2011;105(1):38–43. https://doi.org/10.1038/bjc.2011.215
5. Song H-J, Kim K-M. Pathology of epstein-barr virus-associated gastric carcinoma and its relationship to prognosis. *Gut Liver*. 2011;5(2):143–148. https://doi.org/10.5009/gnl.2011.5.2.143
6. Saito M, Kono K. Landscape of EBV-positive gastric cancer. *Gastric Cancer*. 2021;24(5):983–989. https://doi.org/10.1007/s10120-021-01215-3
7. Kim SY, Park C, Kim H-J, et al. Deregulation of immune response genes in patients with Epstein-Barr virus-associated gastric cancer and outcomes. *Gastroenterology*. 2015;148(1):137–147.e9. https://doi.org/10.1053/j.gastro.2014.09.020
8. Derks S, Nason KS, Liao X, et al. Epithelial PD-L2 expression marks Barrett's esophagus and esophageal adenocarcinoma. *Cancer Immunol Res*. 2015;3(10):1123–1129. https://doi.org/10.1158/2326-6066.CIR-15-0046
9. Salnikov M, Prusinkiewicz MA, Lin S, Ghasemi F, Cecchini MJ, Mymryk JS. Tumor-infiltrating T cells in EBV-associated gastric carcinomas exhibit high levels of multiple markers of activation, effector gene expression, and exhaustion. *Viruses*. 2023;15(1):176. https://doi.org/10.3390/v15010176
10. Shitara K, Fleitas T, Kawakami H, et al. Pan-Asian adapted ESMO Clinical Practice Guidelines for the diagnosis, treatment and follow-up of patients with gastric cancer. *ESMO Open*. 2024;9(2):102226. https://doi.org/10.1016/j.esmoop.2023.102226
11. Shah MA, Kennedy EB, Alarcon-Rozas AE, et al. Immunotherapy and targeted therapy for advanced gastroesophageal cancer: ASCO guideline. *J Clin Oncol*. 2023;41(7):1470–1491. https://doi.org/10.1200/JCO.22.02331
12. Lima Á, Sousa H, Medeiros R, Nobre A, Machado M. PD-L1 expression in EBV associated gastric cancer: a systematic review and meta-analysis. *Discov Oncol*. 2022;13(1):19. https://doi.org/10.1007/s12672-022-00479-0
13. Bai Y, Xie T, Wang Z, et al. Efficacy and predictive biomarkers of immunotherapy in Epstein-Barr virus-associated gastric cancer. *J Immunother cancer*. 2022;10(3):e004080. https://doi.org/10.1136/jitc-2021-004080
14. Brierley JD, Gospodarowicz MK, Wittekind C. *TNM Classification of Malignant Tumours*. 8th ed. Wiley-Blackwell; 2017.
15. Nagtegaal I, Arends MJ, Odze D, Lam A, *WHO Classification of Tumours Editorial Board. Digestive System Tumours*. Vol 1. 5th ed. Ly.; 2019.
16. Salgado R, Denkert C, Demaria S, et al. The evaluation of tumor-infiltrating lymphocytes (TILs) in breast cancer: recommendations by an International TILs Working Group 2014. *Ann Oncol*. 2015;26(2):259–271. https://doi.org/10.1093/annonc/mdu450
17. Angerilli V, Galuppini F, Pennelli G, et al. Epstein-Barr virus associated gastric dysplasia: a new rare entity? *Virchows Arch*. 2022;480(4):939–944. https://doi.org/10.1007/s00428-021-03206-2
18. Mastracci L, Grillo F, Parente P, et al. PD-L1 evaluation in the gastrointestinal tract: from biological rationale to its clinical application. *Pathologica*. 2022;114(5):352–364. https://doi.org/10.32074/1591-951X-803
19. Angerilli V, Fassan M, Parente P, et al. A practical approach for PD-L1 evaluation in gastroesophageal cancer. *Pathologica*. 2023;115(2):57–70. https://doi.org/10.32074/1591-951X-836
20. Fassan M, Kuwata T, Matkowskyj KA, Röcken C, Rüschoff J. Claudin-18.2 immunohistochemical evaluation in gastric and gastroesophageal junction adenocarcinomas to direct targeted therapy: a practical approach. *Mod Pathol*. 2024;37(11):100589. https://doi.org/10.1016/j.modpat.2024.100589
21. Morak M, Ibisler A, Keller G, et al. Comprehensive analysis of the MLH1 promoter region in 480 patients with colorectal cancer and 1150 controls reveals new variants including one with a heritable constitutional MLH1 epimutation. *J Med Genet*. 2018;55(4):240–248. https://doi.org/10.1136/jmedgenet-2017-104744
22. Salnikov MY, MacNeil KM, Mymryk JS. The viral etiology of EBV-associated gastric cancers contributes to their unique pathology, clinical outcomes, treatment responses and immune landscape. *Front Immunol*. 2024;15:1358511. https://doi.org/10.3389/fimmu.2024.1358511
23. Kim ST, Cristescu R, Bass AJ, et al. Comprehensive molecular characterization of clinical responses to PD-1 inhibition in metastatic gastric cancer. *Nat Med*. 2018;24(9):1449–1458. https://doi.org/10.1038/s41591-018-0101-z
24. Agnarelli A, Vella V, Samuels M, Papanastasopoulos P, Giamas G. Incorporating immunotherapy in the management of gastric cancer: molecular and clinical implications. *Cancers (Basel)*. 2022;14(18). https://doi.org/10.3390/cancers14184378
25. Olnes MJ, Martinson HA. Recent advances in immune therapies for gastric cancer. *Cancer Gene Ther*. 2021;28(9):924–934. https://doi.org/10.1038/s41417-021-00310-y
26. Jin X, Liu Z, Yang D, Yin K, Chang X. Recent progress and future perspectives of immunotherapy in advanced gastric cancer. *Front Immunol*. 2022;13:948647. https://doi.org/10.3389/fimmu.2022.948647
27. Comprehensive molecular characterization of gastric adenocarcinoma. *Nature*. 2014;513(7517):202–209. https://doi.org/10.1038/nature13480
28. Nakano H, Saito M, Nakajima S, et al. PD-L1 overexpression in EBV-positive gastric cancer is caused by unique genomic or epigenomic mechanisms. *Sci Rep*. 2021;11(1):1982. https://doi.org/10.1038/s41598-021-81667-w
29. Pellino A, Brignola S, Riello E, et al. Association of CLDN18 protein expression with clinicopathological features and prognosis in advanced gastric and gastroesophageal junction adenocarcinomas. *J Pers Med*. 2021;11(11). https://doi.org/10.3390/jpm11111095
30. Kim T-Y, Kwak Y, Nam SK, et al. Clinicopathological analysis of claudin 18.2 focusing on intratumoral heterogeneity and survival in patients with metastatic or unresectable gastric cancer. *ESMO Open*. 2024;9(12):104000. https://doi.org/10.1016/j.esmoop.2024.104000
31. Kwak Y, Kim T-Y, Nam SK, et al. Clinicopathologic and molecular characterization of stages II-IV gastric cancer with Claudin 18.2 expression. *Oncologist*. 2025;30(2):oyae238. https://doi.org/10.1093/oncolo/oyae238
32. Cyprian FS, Al-Antary N, Al Moustafa A-E. HER-2/Epstein-Barr virus crosstalk in human gastric carcinogenesis: A novel concept of oncogene/oncovirus interaction. *Cell Adh Migr*. 2018;12(1):1–4. https://doi.org/10.1080/19336918.2017.1330244
33. Cristescu R, Lee J, Nebozhyn M, et al. Molecular analysis of gastric cancer identifies subtypes associated with distinct clinical outcomes. *Nat Med*. 2015;21(5):449–456. https://doi.org/10.1038/nm.3850
34. Martinez-Ciarpaglini C, Fleitas-Kanonnikoff T, Gambardella V, et al. Assessing molecular subtypes of gastric cancer: microsatellite unstable and Epstein-Barr virus subtypes. Methods for detection and clinical and pathological implications. *ESMO Open*. 2019;4(3):e000470. https://doi.org/10.1136/esmoopen-2018-000470
35. Businello G, Angerilli V, Parente P, et al. Molecular landscapes of gastric preneoplastic and pre-invasive lesions. *Int J Mol Sci*. 2021;22(18):9950. https://doi.org/10.3390/ijms22189950
36. Fukayama M, Hayashi Y, Iwasaki Y, et al. Epstein-Barr virus-associated gastric carcinoma and Epstein-Barr virus infection of the stomach. *Lab Invest*. 1994;71(1):73–81.